Available online at www.sciencedirect.com
ScienceDirect
Trans. Nonferrous Met. Soc. China 26(2016) 3052−3058
Transactions of Nonferrous Metals Society of China
www.tnmsc.cn

Isothermal section of Al−Ti−Zr ternary system at 1073 K

Kai-li LÜ, Feng YANG, Zhi-yun XIE, Hua-shan LIU, Ge-mei CAI, Zhan-peng JIN

School of Materials Science and Engineering, Central South University, Changsha 410083, China

Received 26 October 2015; accepted 11 April 2016

Abstract: Through alloy sampling combined with diffusion triple technique, phase equilibria in Al−Ti−Zr ternary system at 1073 K were experimentally determined with electron probe microanalysis (EPMA). Experimental results show that there is a solid solution β(Ti,Zr) which dissolves Al up to 16.3% (mole fraction). Ti and Zr can substitute each other in most Ti−Al and Al−Zr binary intermediate phases to a certain degree while the maximum solubility of Zr in Ti_3Al and TiAl reaches up to 17.9% and 4.0% (mole fraction), respectively. The isothermal section consists of 16 single-phased regions, 27 two-phased regions and 14 three-phased regions. No ternary phase was detected.

Key words: Al−Ti−Zr ternary system; phase equilibrium; diffusion triple; solubility

1 Introduction

Coupled with high temperature strength and oxidation resistance, low density and low thermal conductivity make Ti−Al alloys potential replacements to steels and superalloys applied in gas engines and turbines. Among the Ti−Al alloys, γ-TiAl and $TiAl_3$ based intermetallics are important and widely applied alloys [1−6]. Additions of elements have been used to further improve the mechanical performance of titanium aluminium alloys [7−9]. For instance, the addition of Zr improves ductility and toughness, and thus improves processability of Ti−Al base alloys at room temperature [10−12]. Furthermore, the addition of Zr benefits the formation of the Al_3Zr phase, which may serve as potential nucleation core for α(Al), thus results in a homogeneous microstructure with improved machinability of the related Ti−Al alloys [13,14]. To better understand the influence of alloying element Zr in Ti−Al alloys, phase equilibria of the related Al−Ti−Zr system are essential.

The constituent binary systems have been well experimetally studied and thermal dynamically assessed in the literatures. According to Ref. [15], the Ti−Zr binary system is an isomorphous system. The Al−Zr and Ti−Al binary systems were successfully assessed by WANG et al [16] and WITUSIEWICZ et al [17], respectively, with the intermediate compounds included, i.e., Zr_3Al, Zr_2Al, Zr_5Al_3, Zr_3Al_2, Zr_4Al_3, Zr_5Al_4, ZrAl, $ZrAl_3$, $ZrAl_2$, $ZrAl_3$ and $TiAl_3$(h), $TiAl_3$(l), Ti_2Al_5, $TiAl_2$, Ti_3Al_5, TiAl, and Ti_3Al. Information of the stable solid phases in these binary systems is summarized in Table 1.

Phase relations in the Al−Ti−Zr ternary system are far from being accomplished. Only an isothermal section of the Al−Ti−Zr system at 1273 K is available [18]. It is obvious that the phase diagram is the map of material design. In order to assist the design and fabrication of Ti−Al based alloys, extensive investigation of phase equilibria in the Al−Ti−Zr ternary system is necessary. The present work is to determine the isothermal sections of Al−Ti−Zr ternary system at 1073 K experimentally by using diffusion triple technique combined with alloy sampling.

2 Experimental

The present work was to experimentally study the phase relations of Al−Ti−Zr system at 1073 K by diffusion triple and alloy sampling. Ti (99.999%), Al (99.99%) and Zr (99.99%) (mass fraction) were used as starting materials, bought from China New Metal Materials Technology Co., Ltd.. Predetermined amount of each raw material was weighed with analytical

Foundation item: Project (51171210) supported by the National Natural Science Foundation of China; Project (2014CB6644002) supported by the Major State Basic Research Development Program of China

Corresponding author: Hua-shan LIU; Tel: +86-731-88876735; Fax: +86-731-88876692; E-mail: hsliu@csu.edu.cn

DOI: 10.1016/S1003-6326(16)64436-9

Table 1 Stable solid phases in three binary systems [18,19]

Phase	Temperature range/°C	Pearson symbol	Prototype	Lattice parameter/nm			Comment
				a	*b*	*c*	
α(Zr)	<863	hP2	Mg	0.3232	−	0.5148	Pure-Zr at 25 °C
α(Al)	660.452	cF4	Cu	0.4050	−	−	Pure-Al at 25 °C
β(Zr)	1855−863	cI2	W	0.3609	−	−	Pure-Zr at 25 °C
$Ti_3Al(\alpha_2)$	<1164	hP8	Ni_3Sn	0.5806	−	0.4655	Zr-rich
TiAl(γ)	<1463	tP4	CuAu	0.4005	−	0.4070	46.7%−66.5%Al
$TiAl_2(\eta)$	<1199	oC12	$ZrGa_2$	1.2088	0.3946	0.4029	−
Ti_3Al_5	<810	tP32	Ti_3Al_5	1.1293	−	0.4038	−
Ti_2Al_5	1416−990	tP28	Ti_2Al_5	0.3905	−	2.9196	−
$TiAl_3$(h)	950−1393	tI8	$TiAl_3$	0.3849	−	0.8609	74.5%−75% Al
$TiAl_3$(l)	<950	tI32	$TiAl_3$(l)	0.3877	−	3.3828	74.5%−75% Al
$ZrAl_3$	<1580	tI16	$ZrAl_3$	0.4007	−	1.7286	68.5%−70.9%Al
$ZrAl_2$	<1660	hP12	$MgZn_2$	0.5281	−	0.8748	Al-rich
Zr_2Al_3	<1590	oF40	Zr_2Al_3	0.9617	1.3934	0.5584	−
ZrAl	<1275	oC8	CrB	0.3359	−	1.0887	−
Zr_5Al_4	≤1550	−	Ti_5Ga_4	0.8432	−	0.5791	−
Zr_4Al_3	<1020	hP7	Zr_4Al_3	0.5433	−	0.5390	−
Zr_5Al_3	1400−1000	−	W_5Si_3	1.1043	−	0.5392	−
Zr_3Al_2	<1480	tP20	Zr_3Al_2	0.7633	−	0.6996	−
Zr_2Al	≤1215	hP6	Ni_2In	0.4894	−	0.5928	−
Zr_3Al	≤920	cP4	Cu_3Au	0.4372	−	−	−

balance, followed by arc-melted in a water-cooled copper crucible under argon atmosphere with titanium as getter material placed in the arc chamber. To ensure good homogeneity of the samples, all samples were turned over before each melting and re-melted at least 3 times. The mass losses did not exceed 1%.

The method to fabricate diffusion triple can be found in Ref. [20]. The Ti, Zr and deliberately prepared $TiAl_3$ button ingot were machined into the proper shapes (cuboid with 3 mm × 3 mm × 10 mm and cylindrical shells with rectangular openings) through wire-electrode cutting. Surfaces of the metallic pieces were ground, polished, cleaned and then assembled into the geometry shown in Fig. 1. The assembled diffusion triple was then loaded into cans made of commercial purity Ti (schematically shown in Fig. 1(b)), and subjected to hot isostatic pressing (HIP) at 1073 K, 200 MPa for 4 h. The top and bottom caps of the HIP can were electron beam welded.

The obtained diffusion triple and ternary button alloys were sealed in a silica capsule back-filled with high purity argon, and then annealed at 1073 K for 2400 h in a diffusion furnace (temperature error is within ±5 °C). After annealing, the samples were taken out and quenched into water.

The annealed specimens were polished and microstructural investigations of the alloys were carried out using electron probe microanalyser (JXA−8800R, JEOL, Japan). Approach to determination of phase equilibria from diffusion triple relies on the assumption of local equilibrium at the phase interface, and details of the approach can also be found in Ref. [20]. The compositions of equilibrated alloys in this study were the average values of five measurements. Standard deviation of the measured concentration is ±0.6%. The total mass fractions of Al, Zr and Ti in each phase are in the range of 97%−103%, so the effect of reactions between the samples and silica capsules could be neglected.

3 Results and discussion

3.1 Analysis of diffusion triple

Figure 2 illustrates the backscatter electron images of the diffusion triple annealed at 1073 K for 2400 h. During the long-term diffusion treatment, extensive interdiffusion among Al, Ti and Zr took place, and many phases were formed. By performing EPMA analysis, extensive information about phase equilibria was obtained. It can be seen from Fig. 2(a) that several diffusion layers (corresponding to different phases) exist in the tri-junction. By measuring the composition of phases near triple points, 3 three-phased fields could be obtained, including γ(TiAl) + $Zr(Al,Ti)_2$ + β(Ti,Zr), γ(TiAl) + $\alpha_2(Ti_3Al)$ + β(Ti,Zr), $\alpha_2(Ti_3Al)$ + α(Ti) + β(Ti,Zr) and 9 two-phase fields $\varepsilon(TiAl_3)$ + $\eta(TiAl_2)$, $\eta(TiAl_2)$+ γ(TiAl), γ(TiAl) + $\alpha_2(Ti_3Al)$, $\alpha_2(Ti_3Al)$ + α(Ti),

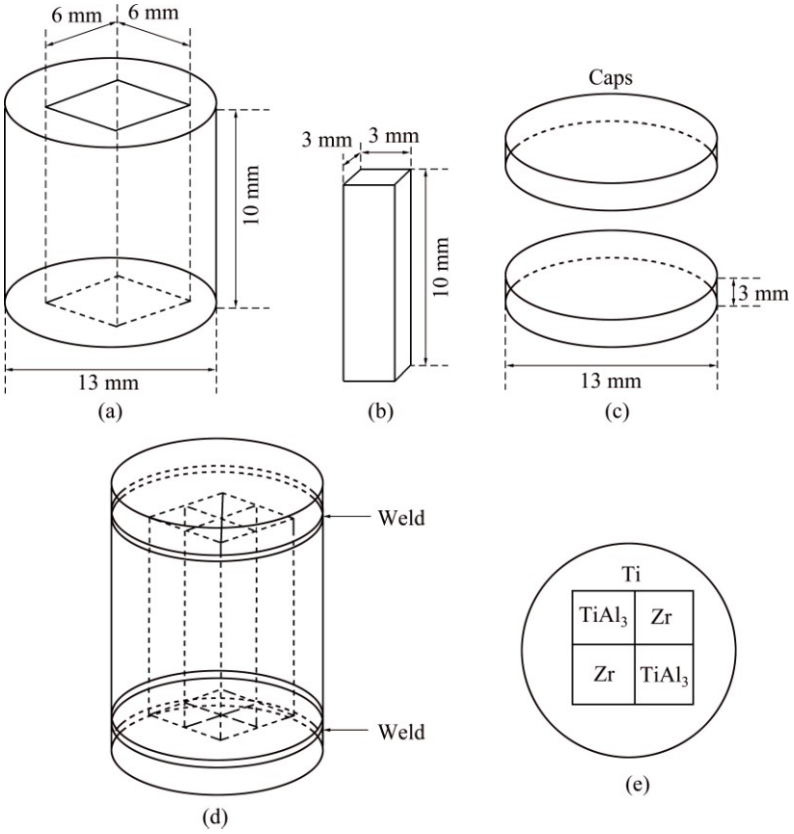

Fig. 1 Schematic illustration of components (a−c), assembly (d), and cross-sectional view (e) of $TiAl_3$−Ti−Zr diffusion triple

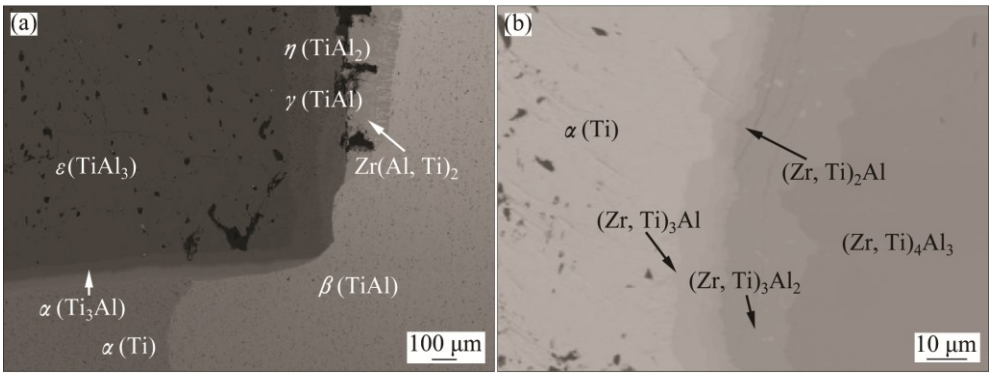

Fig. 2 Backscatter electron SEM image of $TiAl_3$−Ti−Zr diffusion multiple annealed at 1073 K for 2400 h: (a) Tri-junction area; (b) $TiAl_3$−Zr diffusion area

α(Ti) + β(Ti,Zr), α_2(Ti_3Al) + β(Ti,Zr), γ(TiAl) + β(Ti,Zr), $Zr(Al,Ti)_2$ + β(Ti,Zr), γ(TiAl)+$Zr(Al,Ti)_2$. Furthermore, from the $TiAl_3$−Zr diffusion area shown in Fig. 2(b), 5 layers can be distinguished, i.e., α(Zr), $(Zr,Ti)_3Al$, $(Zr,Ti)_2Al$, $(Zr,Ti)_3Al_2$ and $(Zr,Ti)_4Al_3$. Consequently, 4 additional two-phased equilibria, α(Zr) + $(Zr,Ti)_3Al$, $(Zr,Ti)_3Al$ + $(Zr,Ti)_2Al$, $(Zr,Ti)_2Al$ + $(Zr,Ti)_3Al_2$ and $(Zr,Ti)_3Al_2$ + $(Zr,Ti)_4Al_3$, were obtained. The phase equilibria from the diffusion triple are summarized in Table 1.

3.2 Analysis of equilibrated alloys

Back-scattered electron (BSE) images of typical ternary Al–Ti–Zr alloys after annealing at 1073 K are presented in Fig. 3 and Fig. 4. All the samples display a well-defined three-phased or two-phased structure, implying that equilibrium has been reached or nearly reached for the annealed Al−Ti−Zr alloys. In the $Al_{63}Ti_{25}Zr_{12}$ (mole fraction, %, here after) alloy, the three-phased microstructure $Zr(Al,Ti)_2$+η($TiAl_2$)+γ(TiAl) was observed (Fig. 3(a)). As seen in Fig. 3(b), the microstructure of alloy $Al_{50}Ti_{30}Zr_{20}$ consists of dark γ(TiAl) phase, and light gray $Zr(Al,Ti)_2$ phase, indicating that this alloy is located in the two-phased field of γ(TiAl) + $Zr(Al,Ti)_2$. BSE micrograph of the alloy $Al_{60}Ti_5Zr_{35}$ is shown in Fig. 3(c), which is featured with

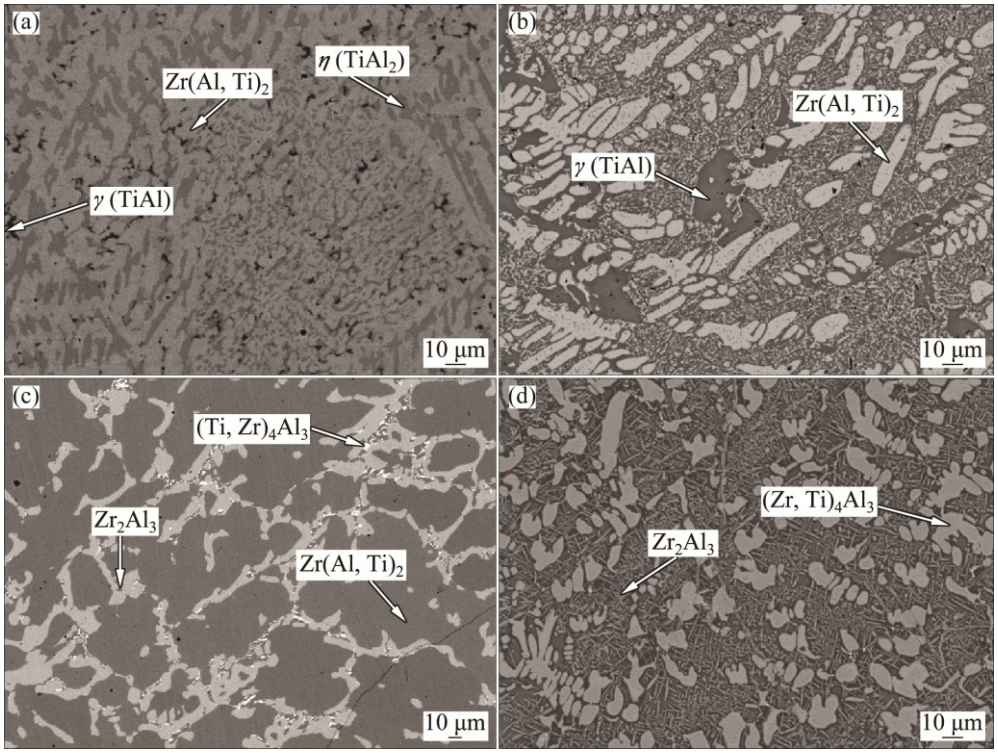

Fig. 3 BSE images of typical Al−Ti−Zr ternary alloys annealed at 1073 K for 2400 h: (a) $Al_{63}Ti_{25}Zr_{12}$ alloy; (b) $Al_{50}Ti_{30}Zr_{20}$ alloy; (c) $Al_{60}Ti_5Zr_{35}$ alloy; (d) $Al_{50}Ti_5Zr_{45}$ alloy

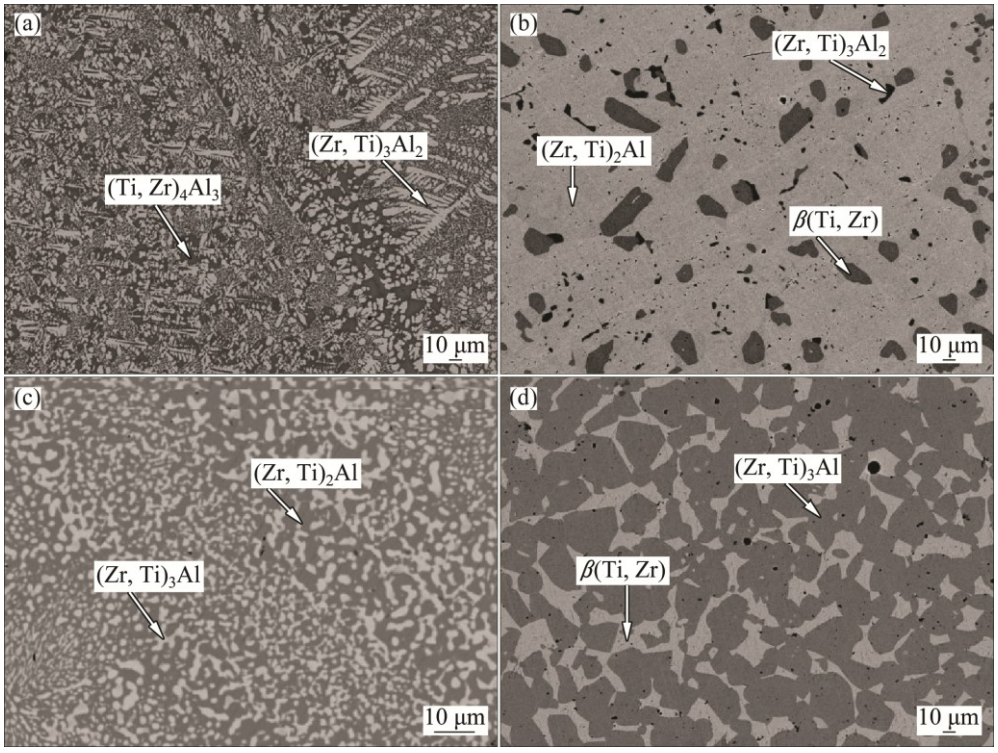

Fig. 4 BSE images of typical Al−Ti−Zr ternary alloys annealed at 1073 K for 2400 h: (a) $Al_{40}Ti_{10}Zr_{50}$ alloy; (b) $Al_{30}Ti_{25}Zr_{45}$ alloy; (c) $Al_{30}Ti_5Zr_{65}$ alloy; (d) $Al_{20}Ti_{10}Zr_{70}$ alloy

a three-phased equilibrium of $Zr(Al,Ti)_2$ + Zr_2Al_3 + $(Zr,Ti)_4Al_3$. Equilibrium between $(Zr,Ti)_3Al_3$ and Zr_2Al_3 was also observed in the alloys $Al_{50}Ti_5Zr_{45}$ (see Fig. 3(d)).

Figure 4(a) shows the microstructure of the alloy $Al_{40}Ti_{10}Zr_{50}$, where the two-phased equilibrium $(Zr,Ti)_4Al_3$ + $(Zr,Ti)_3Al_2$ occurs. The alloy $Al_{30}Ti_{25}Zr_{45}$ contained three phases (see Fig. 4(b)), i.e., the black

$(Zr,Ti)_3Al_2$ phase, the dark gray β(Ti,Zr) phase and the light gray $(Zr,Ti)_2Al$ phase. As is shown in Fig. 4(c), $(Zr,Ti)_3Al$ and $(Zr,Ti)_2Al$ coexist in the $Al_{30}Ti_5Zr_{65}$ alloy. In addition, from Fig. 4(d), it is seen that the alloy $Al_{20}Ti_{10}Zr_{70}$ contains $(Zr,Ti)_3Al$ and β(Ti,Zr) in equilibrium.

3.3 Isothermal section of 1073 K

The measured compositions of all phases in equilibria in the Al−Ti−Zr ternary system at 1073 K are summarized in Table 2. Based on Tables 2 and 3, the isothermal section at 1073 K is constructed as presented in Fig. 5. In the isothermal section, 8 three-phased regions were completely determined, including $\varepsilon(TiAl_3)$ + $(Zr,Ti)Al_3$ + $\eta(TiAl_2)$, $\eta(TiAl_2)$ + $(Zr,Ti)Al_3$ + $Zr(Al,Ti)_2$, γ(TiAl) + $\eta(TiAl_2)$ + $Zr(Al,Ti)_2$, γ(TiAl) + $Zr(Al,Ti)_2$ + β(Ti,Zr), γ(TiAl) + $\alpha_2(Ti_3Al)$ + β(Ti,Zr), $\alpha_2(Ti_3Al)$ + α(Ti) + β(Ti,Zr), $Zr(Al,Ti)_2$ + Zr_2Al_3 + $(Zr,Ti)_4Al_3$ and $(Zr,Ti)_2Al$ + β(Ti,Zr) + $(Zr,Ti)_3Al_2$. Additionally, other 6 three-phased regions, i.e., L + $\varepsilon(TiAl_3)$ + $(Zr,Ti)Al_3$, $Zr(Al,Ti)_2$ + $(Zr,Ti)_4Al_3$ + β(Ti,Zr), $(Zr,Ti)_4Al_3$ + Zr_2Al_3 + ZrAl, $(Zr,Ti)_4Al_3$ + $(Zr,Ti)_3Al_2$ + β(Ti,Zr), $(Zr,Ti)_3Al$ + $(Zr,Ti)_2Al$ + β(Ti,Zr) and $(Zr,Ti)_3Al$ + β(Ti,Zr) + α(Zr) could be further deduced. What's more, According to the Al−Zr binary phase diagram [16], phase ZrAl should be stable at 1073 K. So, it is reasonably deduced that the three-phased region, Zr_2Al_3 + ZrAl + $(Zr, Ti)_4Al_3$, exists at 1073 K.

By the way, in most Ti−Al and Zr−Al binary compounds, Zr atoms and Ti atoms can mutually substitute to a certain degree. The only exception is $Zr(Al,Ti)_2$, whose homogeneity range extends along the isoconcentrate of Zr, meaning substitution of Al by Ti. Moreover, at 1073 K, the maximum solubilities of Ti in $(Zr,Ti)Al_3$, $(Zr,Ti)_2Al$, $(Zr,Ti)_4Al_3$, $(Zr,Ti)_3Al_2$ and $(Zr,Ti)_3Al$ can be up to 12.0%, 11.6%, 13.5%, 14.4% and 8.0% (mole fraction), respectively. Meanwhile, the maximum solubilities of Zr in $TiAl_3$ and $TiAl_2$ were 6.1% and 17.2%, respectively. As to the $Zr(Al,Ti)_2$, the maximum solubility of Ti was 13.8%. Zr_2Al_3 and ZrAl do not show remarkable composition ranges at 1073 K.

Additionally, compared with the isothermal sections of the Al−Ti−Zr system at 1273 K [18], the obvious difference exists in the phase $(Zr,Ti)_5Al_3$, which

Table 2 Equilibrium composition of Al−Ti−Zr ternary system obtained from diffusion couple in present work

Phase equilibria	Mole fraction/%					
Phase 1/Phase 2/Phase 3	Phase 1		Phase 2		Phase 3	
	Ti	Al	Ti	Al	Ti	Al
$\varepsilon(TiAl_3)/\eta(TiAl_2)$	25.5	74.5	33.8	66.2		
$\eta(TiAl_2)/\gamma$(TiAl)	34.3	65.7	45.7	54.3		
γ(TiAl)/$\alpha_2(Ti_3Al)$	49.3	50.5	67.1	32.8		
γ(TiAl)/$\alpha_2(Ti_3Al)$	50.4	47.9	66.2	31.8		
γ(TiAl)/β(Ti, Zr)/$Zr(Al,Ti)_2$	48.1	47.9	51.6	14.9	13.8	53.4
γ(TiAl)/β(Ti, Zr)/$\alpha_2(Ti_3Al)$	49.8	49.2	54.6	14.1	64.2	27.4
$\alpha_2(Ti_3Al)/\beta$(Ti, Zr)	64.3	17.8	63.1	11.6		
$\alpha_2(Ti_3Al)/\beta$(Ti, Zr)	68.1	16.0	71.2	10.2		
$\alpha_2(Ti_3Al)/\beta$(Ti, Zr)/α(Ti)	77.9	20.1	83.8	3.1	94.9	3.0
$Zr(Al,Ti)_2/Zr_2Al_3$	0.8	66.6	0	60		
$(Zr,Ti)_4Al_3/(Zr,Ti)_3Al_2$	0	42.6	0	41.0		
$(Zr,Ti)_3Al_2/(Zr,Ti)_2Al$	0	39.2	0	33.5		
$(Zr,Ti)_2Al/(Zr,Ti)_3Al$	0	33.5	0	25.4		
$(Zr,Ti)_3Al/\alpha$(Zr)	0	25.2	0	6.3		

Table 3 Measured compositions of phases in alloys annealed at 1073 K

Alloy	Phase equilibrium	Mole fraction/%					
	Phase 1/Phase 2/Phase 3	Phase 1		Phase 2		Phase 3	
		Ti	Al	Ti	Al	Ti	Al
$Al_{72}Ti_{23}Zr_5$	$\varepsilon(TiAl_3)/\eta(TiAl_2)$	22.6	74.7	25.1	67.2		
$Al_{74}Ti_{16}Zr_{10}$	$\varepsilon(TiAl_3)/(Zr,Ti)Al_3/\eta(TiAl_2)$	19.3	74.6	12.0	75.1	22.9	65.9
$Al_{70}Ti_{7.5}Zr_{22.5}$	$(Zr,Ti)Al_3/\eta(TiAl_2)/Zr(Al,Ti)_2$	3.9	74.7	16.6	66.2	2.6	66.0
$Al_{63}Ti_{25}Zr_{12}$	$\eta(TiAl_2)/ Zr(Al,Ti)_2/\gamma$(TiAl)	20.7	65.9	4.2	64.3	43.8	52.7
$Al_{50}Ti_{30}Zr_{20}$	γ(TiAl)/$Zr(Al,Ti)_2$	44.1	50.5	11.8	55.1		
$Al_{60}Ti_5Zr_{35}$	$Zr(Al,Ti)_2/(Zr,Ti)_4Al_3/Zr_2Al_3$	5.7	62.2	13.5	42.3	1.3	61.1
$Al_{50}Ti_5Zr_{45}$	$(Zr,Ti)_4Al_3/Zr_2Al_3$	7.7	43.2	0.4	59.3		
$Al_{40}Ti_{10}Zr_{50}$	$(Zr,Ti)_4Al_3/(Zr,Ti)_3Al_2$	5.3	43.1	11.9	39.6		
$Al_{30}Ti_{25}Zr_{45}$	$(Zr,Ti)_3Al_2/(Zr,Ti)_2Al/\beta$(Ti, Zr)	14.4	39.4	11.6	33.5	45.2	16.3
$Al_{30}Ti_5Zr_{65}$	$(Zr,Ti)_2Al/(Zr,Ti)_3Al$	4.1	32.9	6.3	25.0		
$Al_{30}Ti_2Zr_{68}$	$(Zr,Ti)_2Al/(Zr,Ti)_3Al$	1.8	32.9	3.0	25.4		
$Al_{20}Ti_{10}Zr_{70}$	$(Zr,Ti)_3Al/\beta$(Ti,Zr)	8.0	25.2	19.2	8.0		

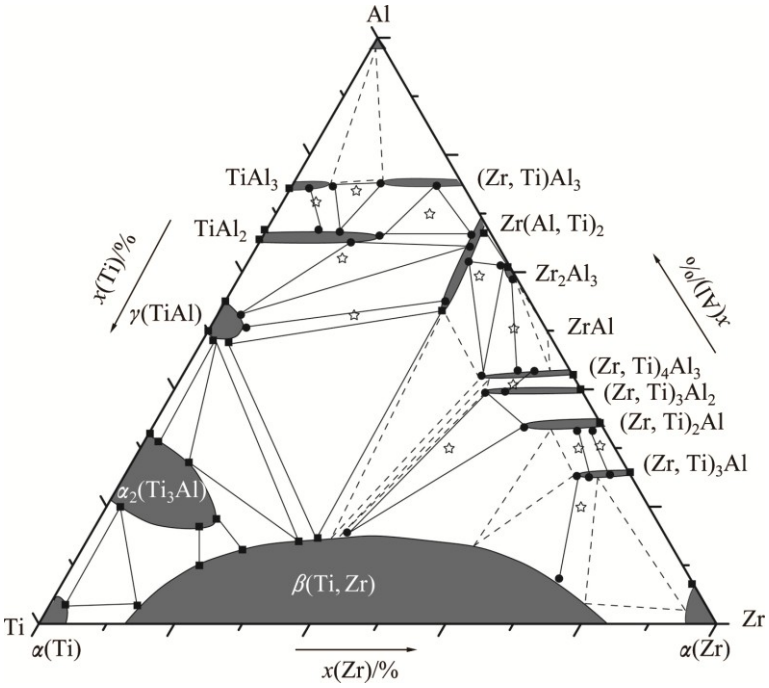

Fig. 5 Experimentally determined isothermal sections of Al−Ti−Zr system at 1073 K: ■ Phase equilibrium determined from diffusion couple; ● Phase equilibrium determined from equilibrated alloys; ☆ Nominal composition of equilibrated alloys

disappears at 1073 K, resulting in the change of the phase relationship related to it. Moreover, with temperature decreasing, solubility of Zr in $\varepsilon(TiAl_3)$ phase decreases from 9.3% to 6.0%, and in γ(TiAl) from 9.0% to 4.0%. As for the BCC solid solution β(Ti, Zr), the maximum solubility of Al was 16.3% at 1073 K, lower than 25.5% at 1273 K [18].

4 Conclusions

1) The isothermal section of the Al−Ti−Zr ternary system at 1073 K was established by analyzing diffusion triple and equilibrated alloys through EPMA.

2) Ti and Zr can substitute each other in most Ti−Al and Al−Zr binary intermediate phases to a certain degree.

3) There is a solid solution β(Ti, Zr) which dissolves up to 16.3% Al. The maximum solubilities of Zr in Ti_3Al and TiAl reach up to 17.9% and 4.0%, respectively.

4) The isothermal section consists of 16 single-phased regions, 27 two-phased regions and 14 three-phased regions. No ternary phase was detected.

References

[1] BAYRAKTAR E, BATHIAS C, XUE H Q, TAO H. On the giga cycle fatigue behaviour of (α_2-Ti_3Al and γ-TiAl) alloy [J]. International Journal of Fatigue, 2004, 26(2): 1263−1275.

[2] KRUZIC J J, CAMPBELL J P, RITCHIE O. On the fatigue behaviour of γ-based titanium aluminides: Role of small cracks [J]. Acta Mater, 1999, 47(3): 801−816.

[3] NIEH T G, HSIUNG L M, WADSWORTH J. Superplastic behavior of a powder metallurgy TiAl alloy with a metastable microstructure [J]. Intermetallics, 1999, 7: 163−170.

[4] WANG Yan, LIU Yong, YANG Guang-yu, LI Hui-zhong, TANG Bei. Microstructure of cast γ-TiAl based alloy solidified from β phase region [J]. Transactions of Nonferrous Metals Society of China, 2011, 21: 215−222.

[5] DENG Tai-qing, YE Lei, SUN Hong-fei, HU Lian-xi, YUAN Shi-jiang. Development of flow stress model for hot deformation of Ti−47%Al alloy [J]. Transactions of Nonferrous Metals Society of China, 2011, 21(S2): s308−s314.

[6] CHEN Wei, GUAN Ying-ping, WANG Zhen-hua. Hot deformation behavior of high Ti6061Al alloy [J]. Transactions of Nonferrous Metals Society of China, 2016, 26: 369−377.

[7] QIU Cong-zhang, LIU Yong, HUANG Lan, ZhANG Wei, LIU Bin, LU Bin. Effect of Fe and Mo additions on microstructure and mechanical properties of TiAl intermetallics [J]. Transactions of Nonferrous Metals Society of China, 2012, 22: 521−527.

[8] KE Y, DUAN H, SUN Y. Effect of yttrium and erbium on the microstructure and mechanical properties of Ti−Al−Nb alloys [J]. Materials Science and Engineering A, 2010, 528: 220−225.

[9] FOX-RABINOVICH G S, WILKINSON D S, VELDHUIS S C, DOSBAEVA G K, WEATHERLY G C. Oxidation resistant Ti−Al−Cr alloy for protective coating applications [J]. Intermetallics, 2006, 14: 189−197.

[10] JIANG X J, ZHOU Y K, FENG Z H, XIA C Q, TAN C L, LIANG S X. Influence of Zr content on β-phase stability in α-type Ti−Al alloys [J]. Materials Science and Engineering A, 2015, 639: 407−411.

[11] FAN G J, SONG X P, QUAN M X, HU Z Q. Mechanical alloying and thermal stability of Al67Ti25M8 (M=Cr, Zr, Cu) [J]. Materials Science and Engineering A , 1997, 231: 111−116.

[12] BELOV N A, ALABIN A N, MATVEEVA I A, ESKIN D G. Effect of Zr additions and annealing temperature on electrical conductivity and hardness of hot rolled Al sheets [J]. Transactions of Nonferrous Metals Society of China, 2015, 25: 2817−2826.

[13] LÜ X Y, GUO E J, ROMETSCH P, WANG L J. Effect of one-step

and two-step homogenization treatments on distribution of Al_3Zr dispersoids in commercial AA7150 aluminium alloy [J]. Transactions of Nonferrous Metals Society of China, 2012, 22: 2645−2651.

[14] WANG F, QIU D, LIU Z l, TAYLOR J, EASTON M, ZHANG M X. Crystallographic study of Al_3Zr and Al_3Nb as grain refiners for Al alloys [J]. Transactions of Nonferrous Metals Society of China, 2014, 24: 2034−2040.

[15] HARI KUMAR K C, WOLLANTS P, DELACY L. Thermodynamic assessment of the Ti−Zr system and calculation of the Nb−Ti−Zr phase diagram [J]. Journal of Alloys and Compounds, 1994, 206: 121−127.

[16] WANG T, JIN Z P, ZHAO J C. Thermodynamic assessment of the Al−Zr binary system [J]. Journal of Phase Equilibria, 2001, 22: 544−551.

[17] WITUSIEWICZ V T, BONDAR A A, HECHT U, REX S, VELIKANOVA T Y. The Al−B−Nb−Ti system: III. Thermodynamic re-evaluation of the constituent binary system Al−Ti [J]. Journal of Alloys and Compounds, 2008, 465: 64−77.

[18] YANG F, XIAO F H, LIU S G, DONG S S, HUANG L H, CHEN Q. Isothermal section of Al−Ti−Zr ternary system at 1273 K [J]. Journal of Alloys and Compounds, 2014, 585: 325−330.

[19] GHOSH G, ASTA M. First-principles calculation of structural energetics of Al−TM (TM = Ti, Zr, Hf) intermetallics [J]. Acta Materialia, 2005, 53: 3225−3252.

[20] KODENSTOV A A, F. BASTIN G, J J. van LOO F. Application of diffusion couples in phase diagram determination [C]//ZHAO Ji-chen, editor. Methods for Phase Diagram Determination. Oxford: Elsevier Science Ltd., 2007: 222−245.

Al−Ti−Zr 三元系 1073 K 等温截面的测定

吕凯丽，杨 冯，谢止云，刘华山，蔡格梅，金展鹏

中南大学 材料科学与工程学院，长沙 410083

摘 要：采用合金样与扩散偶相结合的方法，利用电子探针射线显微分析(EPMA)对 Al−Ti−Zr 三元系的 1073 K 等温截面的相关系进行实验测定。结果表明：截面中存在一个 Al 含量(摩尔分数)达到 16.3%的 β(Ti,Zr)固溶体。Ti 和 Zr 可以在大多数 Al−Zr 和 Ti−Al 二元中间化合物中相互取代。其中，Zr 在 Ti_3Al 和 TiAl 中的最大固溶度分别达到 17.9% 和 4.0%。该等温截面共包含 16 个单相区，27 个两相区和 14 个三相平衡，没有检测到三元化合物。

关键词：Al−Ti−Zr 三元系；相平衡；扩散偶; 固溶度

(Edited by Yun-bin HE)